APPLICATION OF DISCRETE COMPLEX IMAGES METHOD IN CALCULATION OF SOMMERFELD INTEGRALS

Eftim ZDRAVEVSKI[1], Vesna ARNAUTOVSKI-TOSEVA[2] and Leonid GRCEV[3]

Abstract: In this paper, discrete complex images method (DCIM) is applied for calculation of electric field due to a vertical electric (Hertzian) dipole VED in presence of ground. The main objective is to obtain fast and efficient solution of Sommerfeld integrals that arise in the mathematical formulation. The results show very good agreement with exact results. This approach is applied in high-frequency grounding analysis.

Keywords: Discrete complex image method, Sommerfeld integrals, Numerical integration

INTRODUCTION

The Sommerfeld-type integrals (SI) are frequently encountered in a number of electromagnetic problems involving radiation of vertical or horizontal electric dipole. Because of computationally inefficiency of exact integration (numerical difficulties due to oscillations, divergent behavior and singularities), SI has been studied extensively during last decades. Various numerical and analytical techniques have been developed in order to obtain an exact numerical or an approximate solution.

The discrete complex images method (DCIM) was introduced for a large number of radiation problems when analysing multilayered microstrip antennas [1-5]. DCIM was also applied for electrostatic field computation [6].

This paper presents DCIM in analysis of electric field due to VED in presence of conduction half-space. It is a starting point of its application in the electromagnetic modelling of grounding conductors. The main objective is to avoid time consuming numerical integration of Sommerfeld integral, which appears in the exact model of grounding system [9-10].

ELECTRIC FIELD EVALUATION

Sommerfeld integrals for VED in presence of ground

The problem to be solved is presented on fig.1. Consider a VED of unit strength (Il=1) positioned above or within the ground (ground = medium 1, air = medium 2) (characterized by conductivity σ_i and relative permittivity ε_{ri} at source point (x',y',z') and field observed in point (x,y,z), where $\rho = \sqrt{(x-x')^2 + (y-y')^2}$.

Now, we will focus our analysis to evaluation of the z–component of the electric field due to a vertical electric (Herzian) dipole in air or within ground.

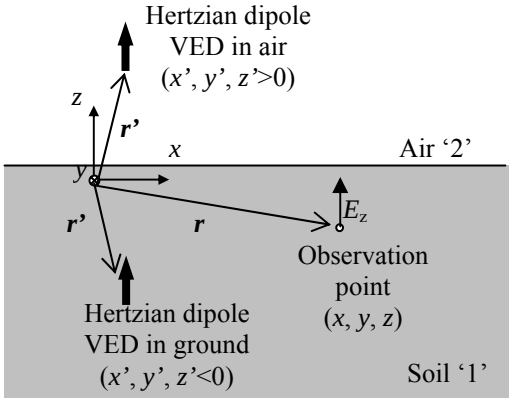

Fig.1 – *Elementary vertical electric dipole VED above or below ground (soil)*

The effect of the air-ground interface is presented by the reflected field from the interface which is formulated as Sommerfeld integral of V type: V_{11} (source below and observer below ground) and V_{22} (source above and observer above ground).

We begin using definition for the fields in terms of the electric type Hertz vectors Π as defined in [7-8]:

- for source and field point in ground (z<0, z'<0)

$$E_{1z}(\rho,z) = \frac{-j\omega\mu_0 Il}{4\pi k_1^2}[(k_1^2 + \frac{\partial^2}{\partial z^2})]\Pi_{11}^V(\rho,z,z') \qquad (1)$$

- for source and field point in air (z>0, z'>0)

$$E_{2z}(\rho,z) = \frac{-j\omega\mu_0 Il}{4\pi k_0^2}[(k_0^2 + \frac{\partial^2}{\partial z^2})]\Pi_{22}^V(\rho,z,z') \qquad (2)$$

where,

$$\Pi_{11}^V = g_d^{11} - g_i^{11} + k_0^2 V_{11} \qquad (3)$$

$$\Pi_{22}^V = g_d^{22} - g_i^{22} + k_1^2 V_{22} \qquad (4)$$

Here, g_d^{11} and g_i^{11} are Green's function of source and image dipole in medium 1 (inedx 11):

$$g_d^{11} = \exp(-jk_1 r_1)/r_1 \qquad (5a)$$

$$g_i^{11} = \exp(-jk_1 r_2)/r_2\,, \qquad (5b)$$

where g_d^{22} and g_i^{22} are Green's function of source and image dipole in medium 2 (index 22):

[1] Faculty of electrical engineering, University Saints Cyril and Methodius, Skopje, 1000 Karpos II bb, Macedonia, E-mail: zeftim@yahoo.com
[2] Faculty of electrical engineering, University Saints Cyril and Methodius, Skopje, 1000 Karpos II bb, Macedonia, E-mail: atvesna@etf.ukim.edu.mk
[3] Faculty of electrical engineering, University Saints Cyril and Methodius, Skopje, 1000 Karpos II bb, Macedonia, E-mail: lgrcev@etf.ukim.edu.mk

$$g_d^{22} = \exp(-jk_0 r_1)/r_1 \quad (6a)$$

$$g_i^{22} = \exp(-jk_0 r_2)/r_2 \,. \quad (6b)$$

Notation r_1 stands for the distance between the source dipole and the observation point in medium 1 or 2, and and r_2 stands for the distance between the image dipole and the observation point in medium 1 or 2.

The reflected field from the interface is formulated as a 'Sommerfeld' component V_{11} or V_{22} [7]:

- for z<0 and z'<0

$$V_{11} = \int_0^\infty \frac{2}{k_1^2\gamma_0 + k_0^2\gamma_1} \exp(-\gamma_1 |z+z'|) J_0(\xi\rho)\xi d\xi \quad (7a)$$

- for z>0 and z'>0.

$$V_{22} = \int_0^\infty \frac{2}{k_1^2\gamma_0 + k_0^2\gamma_1} \exp(-\gamma_0 (z+z')) J_0(\xi\rho)\xi d\xi \quad (7b)$$

Here, k_0 and k_1 are corresponding wave numbers for medium 1 and medium 2 defined by:

$$k_0^2 = \omega^2\mu_0\varepsilon_0 \quad k_1^2 = \omega^2\mu_0\varepsilon_0\underline{\varepsilon} \quad (8)$$

with complex relative dielectric constant:

$$\underline{\varepsilon} = \varepsilon/\varepsilon_0 - j\sigma/(\omega\varepsilon_0) \quad (9)$$

and,

$$\gamma_1 = \sqrt{\xi^2 - k_1^2} \quad \text{and} \quad \gamma_0 = \sqrt{\xi^2 - k_0^2}\,. \quad (10)$$

After some mathematical manipulations, and normalization which eliminates the k_0 dependence, the integrals are rewritten as

$$I_1 = S_0\{\frac{2u_1}{\underline{\varepsilon}u_0 + u_1}\frac{1}{k_0 u_1}\exp(-k_0 u_1 a)\} \quad (11)$$

$$I_2 = S_0\{\frac{2u_0}{\underline{\varepsilon}u_0 + u_1}\frac{1}{k_0 u_0}exp(-k_0 u_0 a)\} \quad (12)$$

where,

$$S_0\{g(\lambda)\} = \int_0^\infty g(\lambda) J_0(\lambda k_0\rho)\lambda d\lambda \quad (13)$$

$$u_1 = \frac{\gamma_1}{k_0} = \sqrt{\lambda^2 - \underline{\varepsilon}} \text{ and } u_0 = \frac{\gamma_0}{k_0} = \sqrt{\lambda^2 - 1} \quad (14)$$

and a=abs(|z+z'|).

DISCRETE COMPLEX IMAGES

The solution of Sommerfeld integrals is based on the approximation of the fractional term in integrals I_1 and I_2 by sum exponentials following the Prony method and the closed form solution of the following integral:

$$I_0 = S_0\{\frac{\exp(-k_0 u_0 a)}{k_0 u_0}\} = \frac{\exp(-jk_0 R)}{R},\ R = \sqrt{\rho^2 + a^2} \quad (15)$$

Our approach has the same foundation as presented in [3], but introduces different path approximation on the complex λ plane (Fig.2).

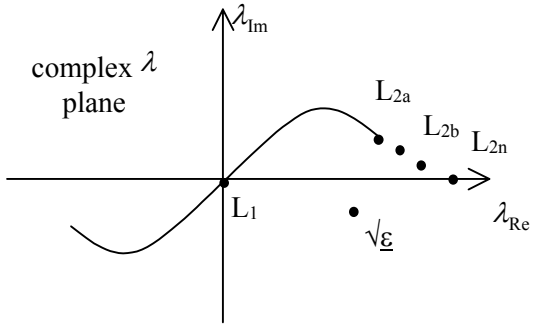

Fig.2 - *Integration path on the complex λ plane*

VED in Air (Medium 2)

In order to obtain the closed-form solution of the integral I_2, it is necessary to obtain an appropriate analytically inverse-transformable presentation. We begin using approximation by a finite sum of complex exponential function of u_0, given by following expression:

$$\frac{2u_0}{\underline{\varepsilon}_r u_0 + u_1} \cong \sum_{i=1}^N a_{2i}\exp(b_{2i}u_0)\,. \quad (16)$$

By this, it is possible to write

$$\begin{aligned} I_2 &= \frac{1}{k_0}\sum_{i=1}^N a_{2i} S_0\{\frac{1}{u_0}\exp(-k_0 u_0 a)\exp(b_{2i}u_0)\} \\ &= \frac{1}{k_0}\sum_{i=1}^N a_{2i}\frac{\exp(-jk_0 R_{2i})}{R_{2i}} \end{aligned} \quad (17)$$

where,

$$R_{2i} = \sqrt{\rho^2 + (a - b_{2i}/k_0)^2}\,,\ i=1,2,\ldots N \quad (18)$$

Here ρ is the radial distance from dipole source to the observation point. Each term in (17) represents one image located at complex distance, in literature well known as a complex image.

Because of the complex character of u_0, an approximated path is obtained by linear transformation related to a real variable t [3]:

$$\sum_{i=1}^N a_{2i}\exp(b_{2i}u_0) \cong \sum_{i=1}^N A_{2i}\exp(B_{2i}t) \quad (19)$$

using linear transformation:

$$u_0 = c_1 t + c_0 \quad \text{where } t \in [0, T_0]\,. \quad (20)$$

Here, c_1 and c_2 are constants to be determined; T_0 is the truncation point of the approximation process, which should be positive and greater than $\sqrt{(\varepsilon_r)}$. It is to emphasise here, that the ending point obtained when t=T_0 is allowed to be elsewhere in the first quadrant (at T_{2a}, or T_{2b}, or.. T_{2n}) along the original path, as presented on fig. 3.

By using, $u_0 = \sqrt{\lambda^2 - 1}$ it may be written:

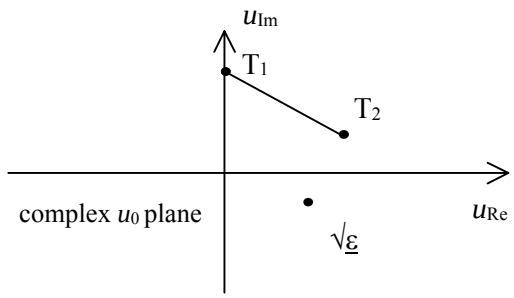

Fig.3 - *Approximation path on the complex u_0 plane*

- if t=0, the starting point L_1=0 in the complex λ plane is transformed to corresponding point T1=u_0(0)=j, on the complex u_0 plane;

- if t=T_0, the ending point λ_2=P+jQ on the complex λ plane is transformed to corresponding point $T_2 = u_0(T_0)=\sqrt{[(P+jQ)^2-1]}$ (P>0, Q>0), on the complex u_0 plane.

The transformed approximated path is shown on Fig.3.

Now, equation (20) can be written as

$$u_0(t) = \frac{\sqrt{(P+jQ)^2-1}}{T_0}t + j(1-\frac{t}{T_0}) \qquad (21)$$

The coefficients P and Q are chosen arbitrarily for an appropriate example. As a special case, we find that the approximation path defined in [3] is determined if P^2=T_0^2+1 and Q=0.

Using (16), (19) and (21) the complex coefficients A_{2i} and B_{2i} are determined. After that, using (19) and (21) the complex coefficients a_{2i} and b_{2i} are obtained as

$$b_{2i} = \frac{B_{2i}}{\sqrt{(P+jQ)^2-1}-j}T_0 \qquad (22)$$

and,

$$a_{2i} = A_{2i}\exp(-jb_{2i})\,. \qquad (23)$$

It is shown that DCIM results are in excellent agreement comparing with exact numerical integration. The calculated error is less than 1%.

VED in Ground (Medium 1)

The closed-form solution of integral I1 is obtained following the same procedure. Firstly, a finite sum of complex exponential function of u1 is introduced as:

$$\frac{2u_1}{\underline{\varepsilon}_r u_0 + u_1} \cong \sum_{i=1}^{N} a_{1i}\exp(b_{1i}u_1) \qquad (24)$$

where a_{1i} and b_{1i} are complex coefficients to be determined.

By this approximation the closed-form solution of the integral I_1 is obtained as

$$I_1 = \frac{1}{k_0}\sum_{i=1}^{N} a_{1i}S_0\{\frac{1}{u_1}Exp[k_0u_1a]Exp[b_{1i}u_1]\} = \frac{1}{k_0}\sum_{i=1}^{N} a_{1i}\frac{Exp[-jk_1R_{1i}]}{R_{1i}} \qquad (25)$$

$$R_{1i} = \sqrt{\rho^2+(a+b_{1i}/k_0)^2}\,,\ i=1,2,..N \qquad (26)$$

By using the exponential approximation it becomes:

$$\sum_{i=1}^{N} a_{1i}\exp(b_{1i}u_1) \cong \sum_{i=1}^{N} A_{1i}\exp(B_{1i}t) \qquad (27)$$

In this case, an approximated path on the complex u1 plane is defined as

$$u_1 = c_1t + c_2 \ \text{ where } \ t \in [0, T_0] \qquad (28)$$

Where c_1 and c_2 are constants to be determined, and T_0 is the truncation point of the approximation process, which should be positive and greater than $\sqrt{(\varepsilon_r)}$.

By using $u_1 = \sqrt{\lambda^2 - \underline{\varepsilon}}$ it may be written:

- the starting point L_1=0 is transformed to corresponding point T_1=u_1(0)=$j\sqrt{(\underline{\varepsilon})}$ on the complex u_1 plane,

- the ending point L_2=U+jW on the complex λ plane is transformed to corresponding point $T_2 = u_1(T_0)=\sqrt{[(U+jW)^2-\underline{\varepsilon}]}$ on the complex u_1 plane.

The transformed approximated path is shown on Fig.4. Now, equation (28) becomes

$$u_1(t) = \frac{\sqrt{(U+jW)^2-\underline{\varepsilon}}}{T_0}t + j\sqrt{\underline{\varepsilon}}(1-\frac{t}{T_0}) \qquad (29)$$

The coefficients U and W are chosen arbitrarily. There are a lot of various constants U and W that may be used to determine a corresponding approximation path. As a special case, we find the approximation path defined in [3] to be determined if U^2=T_0^2+1 and W=0.

Combining equations (24), (27) and (29) we obtain the coefficients A_{1i} and B_{1i}. Now, using (27) and (29) complex coefficients a_{1i} and b_{1i} are obtained as

$$b_{1i} = \frac{B_{1i}}{\sqrt{(U+jW)^2-\sqrt{\underline{\varepsilon}}}-j\sqrt{\underline{\varepsilon}}}T_0 \qquad (30)$$

$$a_{1i} = A_{1i}\exp(-jb_{1i}\sqrt{\underline{\varepsilon}})\,. \qquad (31)$$

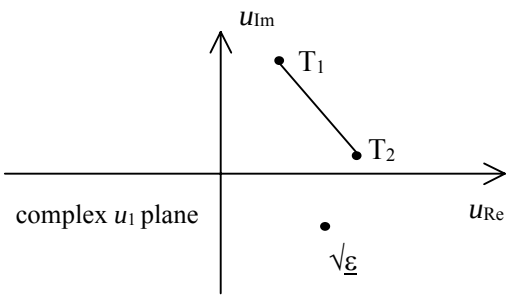

Fig.4 - *Approximation path on the complex u_1 plane*

It is shown that DCIM approximate results are not always acceptable comparing with results of exact numerical integration. It is shown that a vertical distance from source to field point is limiting factor.

NUMERICAL RESULTS

Consider a vertical grounding rod with radius of $0.00025\lambda_0$, extending from a height of $z=0.25\lambda_0$ to a depth of $-0.3\lambda_0$ (λ_0 - free space wavelength). The ground is characterized by relative complex constant $\underline{\varepsilon}$=16-j16. The analysis uses n_g=30 segments for the ground stake, and n_a=25 segments for the upper part of the grounding rod.

To obtain current distribution along the conductor, the calculation of impedance matrix involves Sommerfeld integral to be calculated $\sum_{i=1}^{(n_g+n_a)!} i$ times.

The results of DCIM show that if vertical distance $a=(z+z')$ is larger than $0.05\lambda_0$, the calculated error compared to exact solution is less than 3%.

It means that exact numerical integration can be reduced to $\sum_{i=1}^{10!} i$ times. The results presented in Table I are obtained using N=9 discrete complex images, with T_0=16, and constants U=1.273 and W=2.489.

Table I

Differences in % comparing exact numerical solution of Sommerfeld integrals and DCIM results.

f (MHz)	$a=.05\lambda_0$	$a=.01\lambda_0$	$a=0.3\lambda_0$
5	3.1%	0.65%	0.0173%
10	2.58%	0.42%	0.0044%
15	2.56%	0.41%	0.0040%
20	2.54%	0.40%	0.0042%
50	2.53%	0.398%	0.0039%
100	2.53%	0.397%	0.0038%

CONCLUSION

In this paper discrete complex images method (DCIM) is used to obtain approximate fast solution of Sommerfeld integral that appears in the analysis of VED in presence of air-ground half-space. The results may be used in modelling vertical grounding electrode penetrating the ground. Thus, the time consuming direct numerical evaluation of the Sommerfield-type integrals is completely or partially avoided.

REFERENCES

[1] Y.L.Chow, J.J.Yang, D.G.Fang, G.E.Howard, "A closed-form spatial Green's function for the thic microstrip substrate," *IEEE Transactions on Microwave Theory and Techniques*, Vol. 39, No.3, pp.588-592, March 1991.

[2] D.G.Fang, J.J.Yang, G.Y.Delisle, "Descrete image theory for horizontal electric dipoles in a multilayerd medium," *IEE Proceedings*, Vol.135, Pt.H. No.5, pp.297-303, October 1988.

[3] J.J.Yang, Y.L.Chow, D.G.Fang, "Descrete complex images of a three-dimensional dipole above and within a lossy ground," *IEE Proceedings*, Vol.138, No.4, pp.319-326, August 1991.

[4] R.M.Shubair, Y.L.Chow, "A simple and accurate complex image interpretation of vertical antennas present in contiguous dielectric half-spaces," *IEEE Transactions on Antennas and Propagation*, Vol.41, pp.806-812, June 1993.

[5] B.Popovski, V.Arnautovski, "A Closed-form Spatial Electric Green's Function for the Anisotropic Grounded Layer", JBMSAEM 1998, Sofija, Bulgaria.

[6] Y.L.Chow, J.J.Yang, G.E.Howard, "Complex Images for Electrostatics Field Computation in Multilayered Media," *IEEE Transactions on Microwave Theory and Techniques*, Vol. 39, No.7, pp. 1120-1125, July 1991.

[7] G.J.Burke, E.K.Miller, "Modeling Antennas Near to and penetrating a Lossy Interface", *ASP*-32, No.10, Oct.1984, pp.1040-1049.

[8] Banos A. "Dipole radiation in a presence of a conducting half-space", *Pargamon Press*, London, 1966.

[9] L. Grcev and V. Arnautovski, "Computer Model for Electromagnetic Transients in Thin Wire Structures Above, Below and Penetrating the Earth", EMF2000, Gent, Belgium, 2000.

[10] L. Grcev, "Dynamic Behavior of Grounding Systems", Proc. Int. Zurich Symp. on Electromagnetic Compatibility (EMC Zurich 2003), Zurich, Switzerland, Paper 106P6, pp. 569-574.

Eftim Zdravevski was born in Radovish, Macedonia on July 17, 1984. He studied mathematical high school "Kosta Susinov" in Radovish, from 1999 to 2003. During his high school years he has participated in many math and informatics competitions and has won several awards. In 2003 he was a member of the Macedonian Olympiad Team in informatics team that participated in The Balkan Olympiad in Informatics in Iasi, Romania. In June, 2006 he has finished the third year of his studies of computer science at Faculty od Electrical Engineering, "Ss. Cyril and Methodius" University in Skopje, Macedonia. Eftim Zdravevski is a MENSA member since November, 2004.